iScience

CellPress
OPEN ACCESS

Article

Regorafenib promotes antitumor progression in melanoma by reducing RRM2

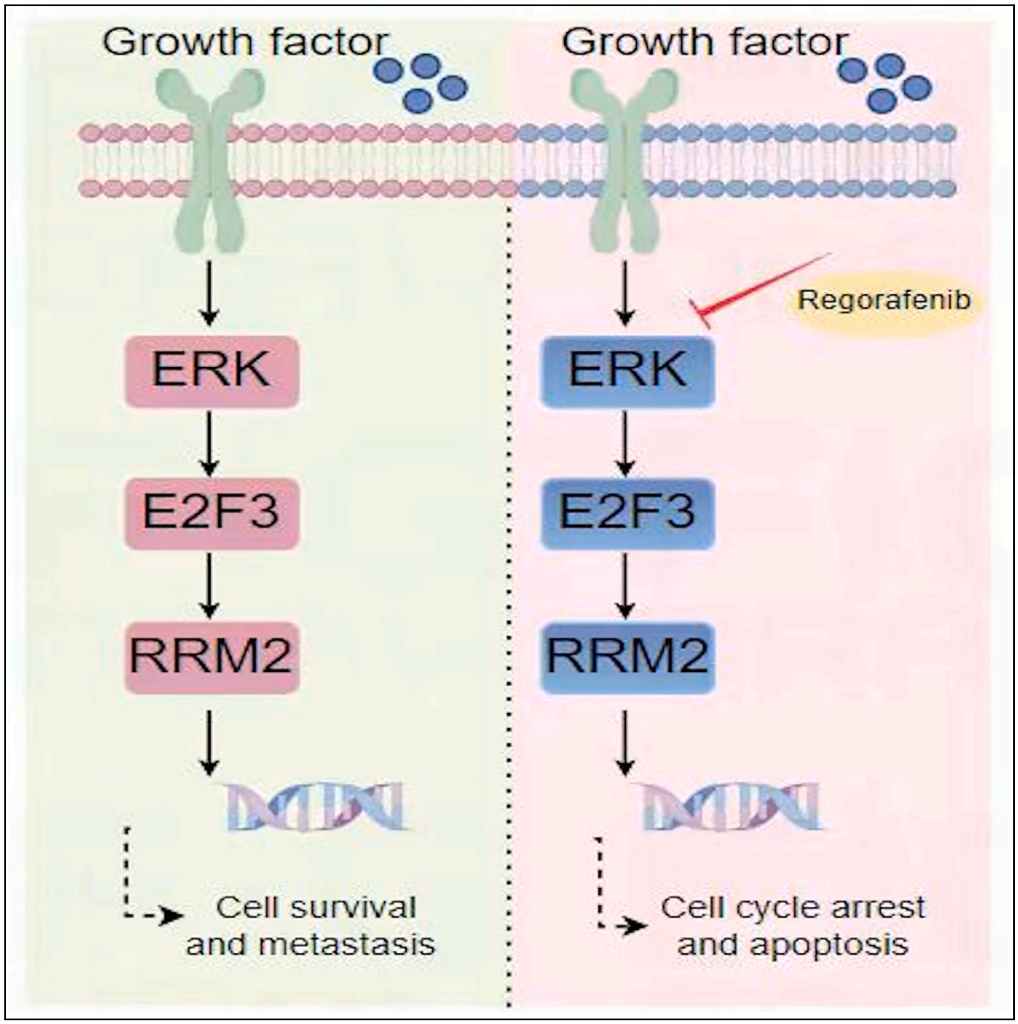

Xiuyun Xuan, Yanqiu Li, Changzheng Huang, Yong Zhang

xiuyunxuanlw@163.com (X.X.)
155212476@qq.com (Y.L.)
hcz0501@126.com (C.H.)
61112426@qq.com (Y.Z.)

Highlights

Regorafenib limits the malignancy but prompts apoptosis of melanoma cells

RRM2 is identified to be the downstream target of regorafenib in melanoma

Regorafenib promotes anti-melanoma progression through ERK/E2F3 signaling

Xuan et al., iScience 27, 110993
October 18, 2024
https://doi.org/10.1016/j.isci.2024.110993

iScience

CellPress
OPEN ACCESS

Article

Regorafenib promotes antitumor progression in melanoma by reducing RRM2

Xiuyun Xuan,[1,4,*] Yanqiu Li,[2,*] Changzheng Huang,[3,*] and Yong Zhang[1,*]

SUMMARY

Melanoma is a malignant tumor with a terrible prognosis. Although so many therapies are used for melanoma, the overall survival rate is still poor globally. Novel therapies are still required. In our study, the role and potential mechanism of regorafenib in melanoma are explored. Regorafenib has the ability to limit the growth, invasion, and metastasis of melanoma cells but to upregulate apoptosis-prompting markers (cleaved-PARP and Bax). RRM2 is identified to be the downstream target of regorafenib by RNA sequencing. In addition, we discovered that RRM2 inhibition and regorafenib have comparable effects on melanoma cells. Rescue experiments showed that RRM2 is crucial in regulating regorafenib's anti-melanoma progression. Moreover, ERK/E2F3 signaling influences regorafenib's ability to suppress melanoma cell growth. Ultimately, regorafenib significantly inhibits tumor growth *in vivo*. In conclusion, our finding demonstrated that regorafenib promotes antitumor progression in melanoma by reducing RRM2.

INTRODUCTION

Melanoma is a malignant tumor derived from transformed melanocytes, and its incidence continues to rise worldwide.[1] As therapeutic approaches, such as surgery, chemotherapy, biological therapy, skin-directed therapy, and radiotherapy, are widely utilized to treat melanoma.[2–4] However, the effectiveness of these therapies is constrained by postoperative recurrence, low sensitivity, toxic and side effects, and medication resistance. Therefore, alternatives to conventional treatments are desperately needed for melanoma.

Due to its tendency to metastasize at an early stage, melanoma has a relatively dismal prognosis. Metastasis is a complex process which requires high vascularization. Hence, inhibition angiogenesis may become a promising therapeutic approach.[5] As we all know, vascular endothelial growth factor (VEGF) and its receptors (VEGFRs) are essential for the angiogenesis process.[6–8] Notably, regorafenib acts as a small-molecule inhibitor of multiple protein kinases, including VEGFR1/2/3 and PDGFR-β, and is reported to be able to inhibit tumor angiogenesis and growth and stroma formation.[9–11] Nevertheless, the exact mechanisms of regorafenib suppressing cancer pathogenesis have not been fully elucidated. Several clinical studies have reported that regorafenib appears to have extensive anticancer action in various solid tumors. For instance, in colorectal cancer and advanced gastrointestinal stromal tumors (GISTs), regorafenib has been shown to improve overall survival and progression-free-survival of cancer patients.[12,13] However, researches on regorafenib usage in melanoma patients are limited.

Ribonucleotide reductase (RR), consisting of two subunits named RRM1 and RRM2, is required for DNA repair and replication.[14] RRM1 protein expression is essentially stable throughout a cell's lifespan, however RRM2 protein expression fluctuates dynamically in response to the stimulation of the cell.[15] RRM2 has been shown to participate in the regulation and modification of proteins.[16–18] Moreover, RRM2 plays a critical role in the etiology of cancer and is a regulator of some oncogenes.[19] In addition, RRM2 is also a potential biomarker of many cancers, such as bladder cancer and lung adenocarcinoma.[20,21] Targeting RRM2 in melanoma seems a novel strategy.[22,23] However, whether and how regorafenib reducing RRM2 to promote antitumor progression in melanoma is still not clear.

Thus, our study aimed to explore the underlying roles and mechanism of regorafenib in melanoma. Our finding demonstrated that regorafenib induces melanoma cell death by inhibiting the proliferation, invasion, and metastasis and prompting the apoptosis of cancer cells. Mechanistically, regorafenib decreases the expressions of RRM2 and ERK/E2F3 signaling in melanoma cells. As a result, our study offered evidence of regorafenib against melanoma and suggested that it may be a valuable treatment option for melanoma.

RESULTS

Regorafenib significantly inhibits melanoma cells growth

To explore whether regorafenib affected the growth and proliferation of melanoma cells, melanoma cells (A2058, SK-Mel-2, SK-Mel-28, and MUM-2B) were treated with 0, 2.5, 5, or 10 μM regorafenib for 24 h or 48 h. CCK8 cytotoxicity assay showed that regorafenib has an obvious cytotoxicity in a concentration- and time-dependent manner (Figure 1A). However, regorafenib does not appear to be cytotoxic to normal

[1]Department of Dermatology, Tongji Hospital, Tongji Medical College, Huazhong University of Science and Technology, Wuhan 430022, Hubei, China
[2]Department of Dermatology, Hubei NO.3 People's Hospital of Jianghan University, Wuhan 430033, Hubei, China
[3]Department of Dermatology, Union Hospital, Tongji Medical College, Huazhong University of Science and Technology, Wuhan 430022, Hubei, China
[4]Lead contact
*Correspondence: xiuyunxuanlw@163.com (X.X.), 155212476@qq.com (Y.L.), hcz0501@126.com (C.H.), 61112426@qq.com (Y.Z.)
https://doi.org/10.1016/j.isci.2024.110993

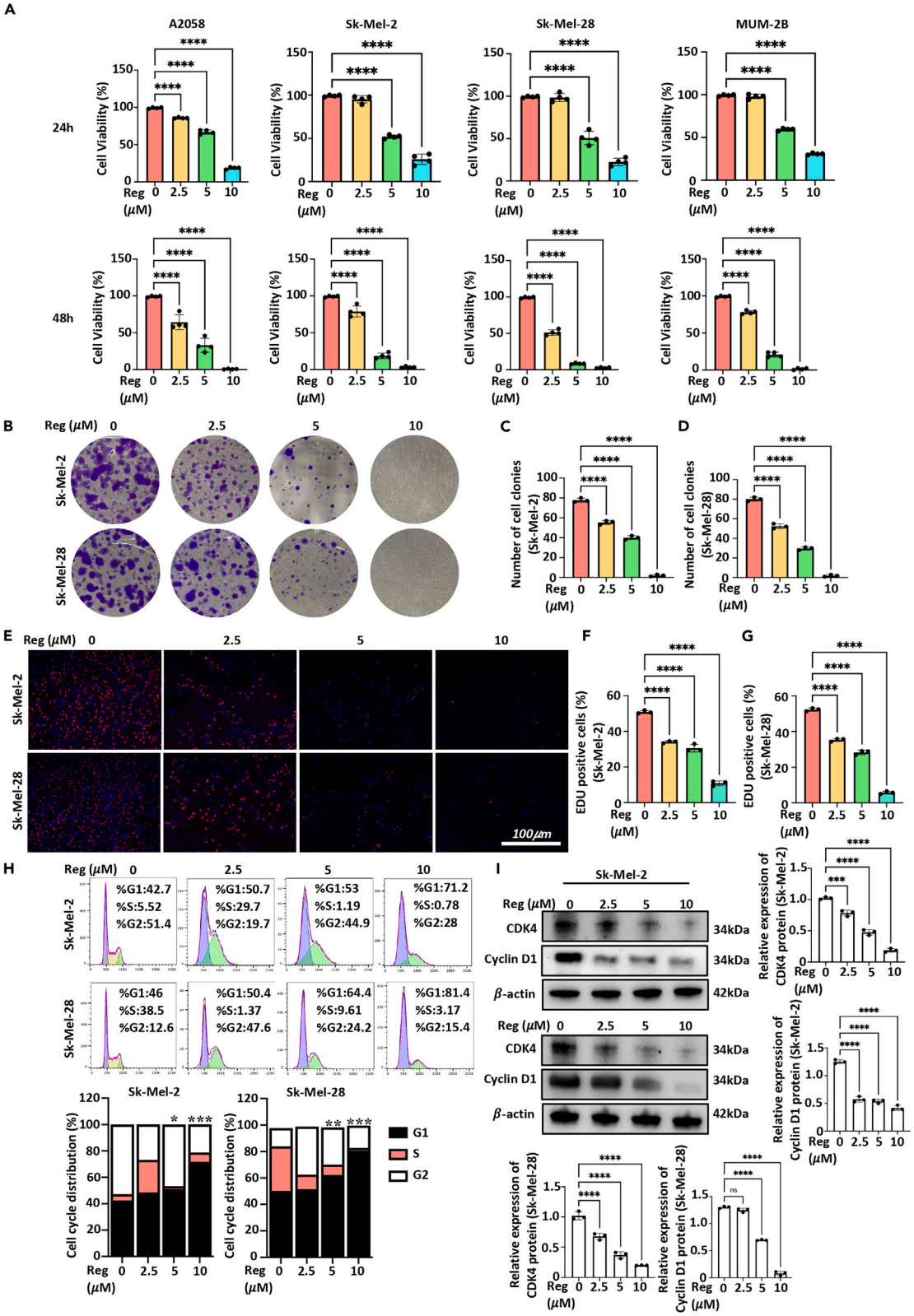
A
A2058
Sk-Mel-2
Sk-Mel-28
MUM-2B
24h
48h
Cell Viability (%)
Reg (μM) 0 2.5 5 10
B
Reg (μM) 0 2.5 5 10
Sk-Mel-2
Sk-Mel-28
C
Number of cell clonies (Sk-Mel-2)
D
Number of cell clonies (Sk-Mel-28)
E
Reg (μM) 0 2.5 5 10
Sk-Mel-2
Sk-Mel-28
100μm
F
EDU positive cells (%) (Sk-Mel-2)
G
EDU positive cells (%) (Sk-Mel-28)
H
Reg (μM) 0 2.5 5 10
Sk-Mel-2
%G1:42.7 %S:5.52 %G2:51.4
%G1:50.7 %S:29.7 %G2:19.7
%G1:53 %S:1.19 %G2:44.9
%G1:71.2 %S:0.78 %G2:28
Sk-Mel-28
%G1:46 %S:38.5 %G2:12.6
%G1:50.4 %S:1.37 %G2:47.6
%G1:64.4 %S:9.61 %G2:24.2
%G1:81.4 %S:3.17 %G2:15.4
Sk-Mel-2
Sk-Mel-28
Cell cycle distribution (%)
G1
S
G2
I
Sk-Mel-2
Reg (μM) 0 2.5 5 10
CDK4
Cyclin D1
β-actin
34kDa
34kDa
42kDa
Relative expression of CDK4 protein (Sk-Mel-2)
Relative expression of Cyclin D1 protein (Sk-Mel-2)
Sk-Mel-28
Relative expression of CDK4 protein (Sk-Mel-28)
Relative expression of Cyclin D1 protein (Sk-Mel-28)
ns

Figure 1. Regorafenib significantly inhibited melanoma cells growth

(A) Regorafenib had an obvious cytotoxicity on melanoma cells in a concentration- and time-dependent manner.

(B–G) Regorafenib markedly inhibited melanoma cells growth by cell colony formation (B–D) and EDU staining (E–G. Scale bar: 100 μm).

(H) Dose-dependent regorafenib treatment blocked the cell cycle transition from G1 to S in Sk-Mel-2/28 cell lines.

(I) The levels of CDK4 and cyclin D1, G1 phase-regulated proteins, were reduced by regorafenib in Sk-Mel-2/28 cell lines. Reg: regorafenib. *$p < 0.05$, **$p < 0.01$, ***$p < 0.001$, ****$p < 0.0001$. Data are represented as mean ± SEM. Similar results were obtained in two additional independent experiments. Data are represented as mean ± SEM.

human skin cells, including human epidermal melanocytes (HEM) and Hacat cells (Figure S1). Notably, we observed that regorafenib at 2.5, 5, and 10 μM after 48 h treatment induces significant inhibition of cell proliferation. Thus, regorafenib treatment for 48 h was used for further experiments. Meanwhile, 10 μM regorafenib have slightly weak toxicity on Sk-Mel-2 and Sk-Mel-28 cell lines compared with A2058 and MUM-2B, thus we chose Sk-Mel-2 and Sk-Mel-28 cell lines for further experiments. Consistently, regorafenib markedly reduces the proportion of EdU-positive proliferative cells and the number of cell colony, indicating that regorafenib could slow the proliferation of melanoma cells (Figures 1B–1G).

To further explore the mechanism of regorafenib-induced inhibition of proliferation in melanoma cells, cell cycle distributions of Sk-Mel-2 and Sk-Mel-28 cells were examined by FCM following indicated concentrations of regorafenib treatment. Our results showed that dose-dependent regorafenib treatment blocks the cell cycle transition from G1 to S in both melanoma cell lines (Figure 1H). In addition, the impact of regorafenib on cell cycle-related factors was further analyzed by western blot. As shown in Figure 1I, the levels of CDK4 and cyclin D1, G1 phase-regulated proteins, are reduced by regorafenib in Sk-Mel-2 and Sk-Mel-28 cell lines.

Regorafenib suppresses the invasive and migrated capacities of melanoma cells

To examine the effects of regorafenib on the invasion and migration of melanoma cells, transwell assay and wound healing were performed. Transwell assay pre-coated extracellular matrix gels showed that regorafenib reduces the number of invaded cells (Figure 2A). Moreover, transwell assay without extracellular matrix gels further indicated that regorafenib considerably decreases the numbers of migrated cells, compared to that of the control group (Figure 2B). In addition, our results suggested that regorafenib restrains wound healing of melanoma cells in a concertation-dependent manner (Figures 2C and 2D). These results indicated that regorafenib has the ability to prevent melanoma cells from invading and migrating.

Regorafenib induces apoptosis in *melanoma cells*

After melanoma cells were treated with indicated concentration of regorafenib for 48 h, we observed increased floating round-shaped apoptotic cells, suggesting that regorafenib may trigger the apoptosis of melanoma cells. To confirm this, the expressions of apoptosis-associated proteins (such as cleaved-PARP, Bax, and Bcl-2) were examined. Western blot analysis and immunofluorescence staining revealed that the expression of Bax and cleaved-PARP are increased, while the expression of Bcl-2 is decreased in SK-Mel-2 and SK-Mel-28 cell lines treated by regorafenib (Figures 3A and 3B). In addition, Annexin V/7-AAD double staining assay was conducted by flow cytometry (FCM) to detect the apoptotic cells after regorafenib treatment. FCM results showed that the frequencies of apoptotic cells in regorafenib-treated group are much higher than that in control group (Figure 3C). These results indicated that regorafenib induces apoptosis in melanoma cells.

RRM2 is the downstream target of regorafenib

To explore the precise mechanism and identify the changes in mRNA level between regorafenib treatment and control group, the transcriptomes of three regorafenib treatment and three control samples were analyzed using RNA-seq. To confirm the reliability of regorafenib treatment and control samples, these six samples were analyzed by principal-component analysis (PCA). PCA suggested a clear distinction between regorafenib treatment and control samples (Figures 4A and 4B), indicating that the differential mRNA expressions contain crucial information to distinguish these two conditions. Next, differentially expressed genes (DEGs) between regorafenib treatment and control samples were determined. An adjusted p value <0.05 and $|\log_2 FC| \geq 1$ were established as the cutoff criteria. 1,502 upregulated and 780 downregulated DEGs were identified in regorafenib treatment samples (Figure 4C). After treatment with regorafenib, the expression of certain DEGs may increase or decrease. Here, we randomly selected downregulated DEGs for further analysis. Downregulated DEGs were used for enrichment analysis, including Gene Ontology (GO) and Kyoto Encyclopedia of Genes and Genomes (KEGG). Enrichment analysis revealed that downregulated genes in regorafenib treatment samples are enriched in several pathways, such as angiogenesis, response to bacterium, receptor regulator activity, receptor ligand activity, proximal promoter sequence-specific DNA binding, transcriptional activator activity, and MAPK signaling pathway (Figures 4D and 4E). These results suggested that regorafenib may inhibit the pathogenesis of melanoma through preventing the transcriptomic changes of associated genes. To identify crucial regulators in the course of melanoma, the public melanoma datasets (Database: GSE7553) was performed for a comprehensive analysis, which revealed that there are 389 upregulated genes and 1,467 downregulated genes in melanoma specimens. Through combining analysis of our RNA-seq_down genes and GSE7553_up genes, we ultimately identified 25 overlapping DEGs (ODEGs) which probably took part in the inhibition of regorafenib on melanoma development (Figures 4F; Table S2). Under the premise of $|\log_2 FC| \geq 1$, the genes with too many or too few researches in melanoma were removed. Finally, only four genes (*GINS2*, *RRM2*, *FEN1*, and *UHRF1*) were obtained. Moreover, their mRNA levels were examined when melanoma cells were treated with different concentrations of regorafenib. Our results revealed that only RRM2 mRNA changes are logical (Figure S2). Meanwhile,

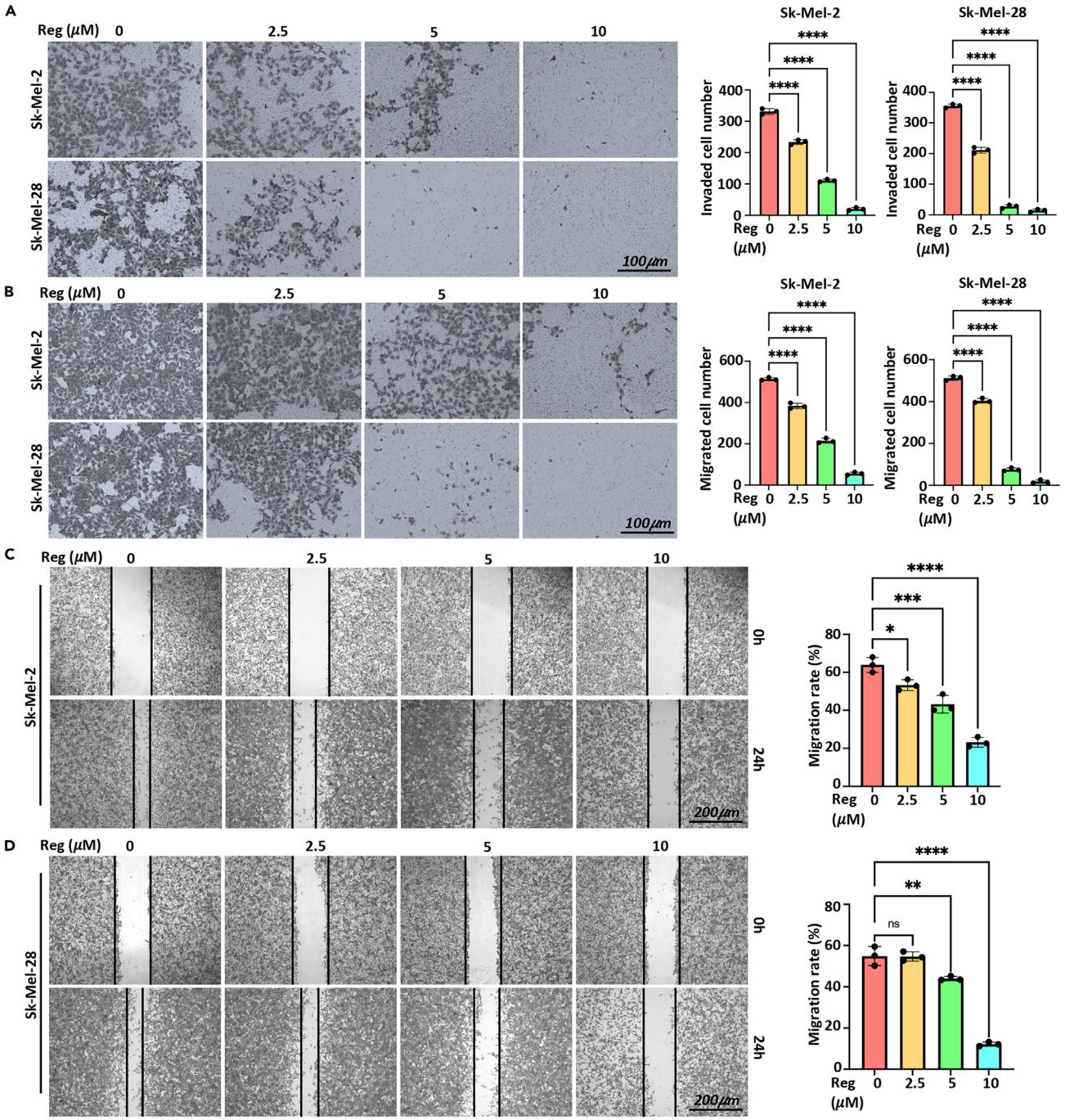

Figure 2. Regorafenib suppressed the invasive and migrated capacities of melanoma cells

(A) Regorafenib reduced the proportion of invaded cells.

(B–D) Regorafenib significantly decreased the quantity of migrating cells and inhibited melanoma cell wound repair. Reg: regorafenib. *$p < 0.05$, **$p < 0.01$, ***$p < 0.001$, ****$p < 0.0001$. Data are represented as mean ± SEM. Similar results were obtained in two additional independent experiments. (A + B) Scale bar: 100 μm. (C + D) Scale bar: 200 μm.

researches showed that targeting RRM2 has been suggested to be a viable therapeutic for melanoma,[22,23] which clued us that RRM2 may have an important role in the etiology of melanoma. Thus, RRM2 was selected to be the downstream target of regorafenib. Here, we want to know whether RRM2 is involved in the inhibition of regorafenib on the malignancy of melanoma. Our results indicated that varying doses of regorafenib decrease the expressions of RRM2 protein in melanoma cells (Figure 4G). In addition, molecular docking was performed to identify the

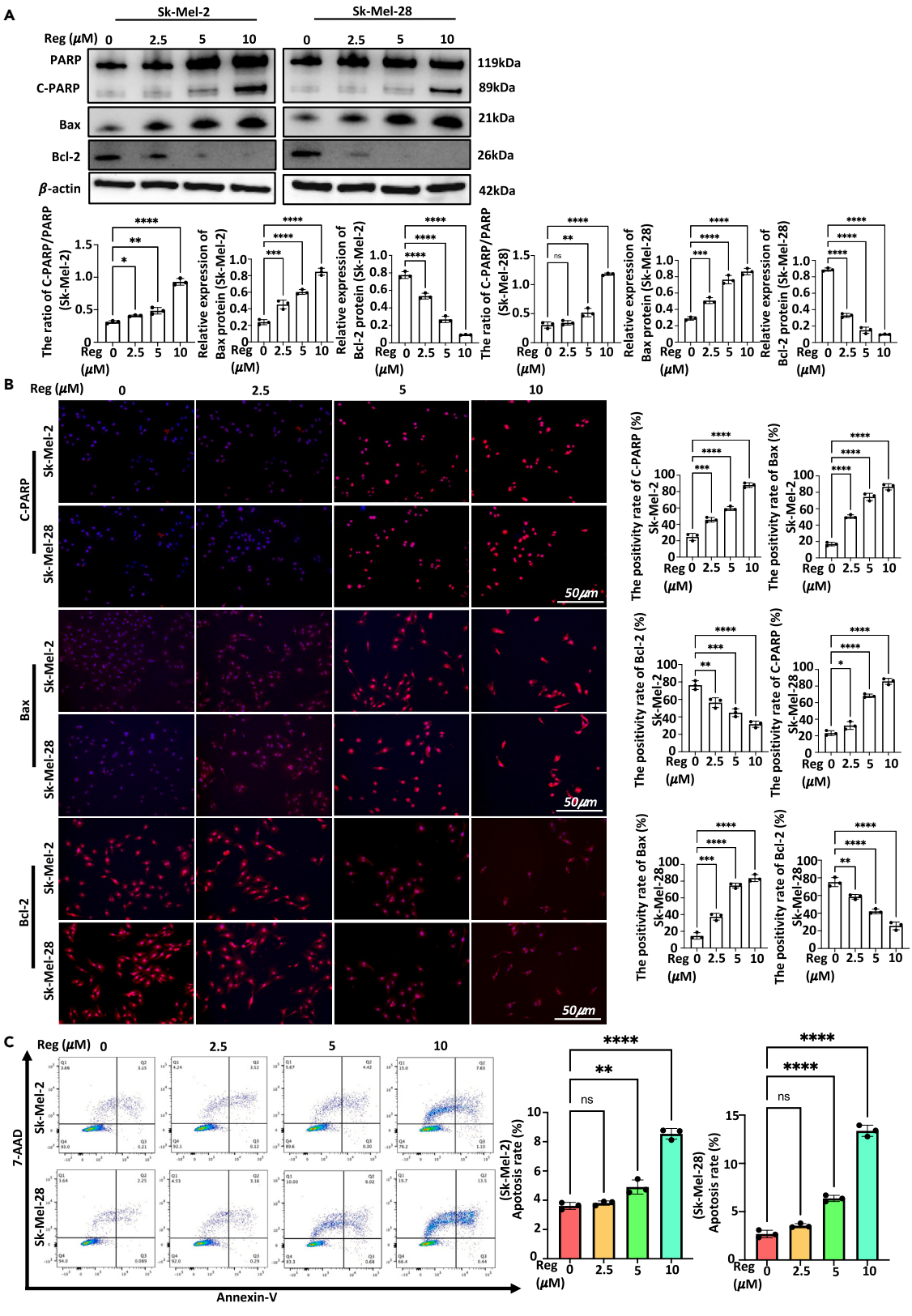
A
Sk-Mel-2
Sk-Mel-28
Reg (μM) 0 2.5 5 10
PARP
C-PARP
Bax
Bcl-2
β-actin
119kDa
89kDa
21kDa
26kDa
42kDa
The ratio of C-PARP/PARP (Sk-Mel-2)
Relative expression of Bax protein (Sk-Mel-2)
Relative expression of Bcl-2 protein (Sk-Mel-2)
The ratio of C-PARP/PARP (Sk-Mel-28)
Relative expression of Bax protein (Sk-Mel-28)
Relative expression of Bcl-2 protein (Sk-Mel-28)
B
C-PARP
Bax
Bcl-2
50μm
The positivity rate of C-PARP (%)
The positivity rate of Bax (%)
The positivity rate of Bcl-2 (%)
C
7-AAD
Annexin-V
(Sk-Mel-2) Apotosis rate (%)
(Sk-Mel-28) Apotosis rate (%)

Figure 3. Regorafenib induced apoptosis in melanoma cells

(A and B) The expression of Bax and cleaved-PARP were increased, while the expression of Bcl-2 was decreased after melanoma cells were treated with regorafenib for 48 h, which were confirmed by western blot analysis (A) and immunofluorescence staining (B, Scale bar: 50 μm).

(C) Regorafenib increased the frequencies of apoptotic cells by FCM. Reg: regorafenib. $^{**}p < 0.01$, $^{****}p < 0.0001$. Data are represented as mean ± SEM. Similar results were obtained in two additional independent experiments.

interaction between the RRM2 protein (Protein Data Bank (PDB) code: 2uw2) and regorafenib, as shown in Figure 4H, the docking results showed that RRM2 and regorafenib have strong binding energy with −6.25 kcal/mol. Regorafenib interacts with the residues ASP-271 and SER-263 through the formation of hydrogen bonds. All of the results suggested that RRM2 is a participant in the repression of regorafenib on melanoma cells and a target of regorafenib in melanoma.

Depletion of RRM2 alleviates the malignancy of melanoma cells

Although it has been claimed that targeting RRM2 is a potential therapeutic for melanoma, the functions of RRM2 in the advancement of melanoma need to be better elaborated. Thus, to investigate the role of RRM2 in melanoma pathogenesis, RRM2 expression was eliminated in Sk-Mel-2 and Sk-Mel-28 cell lines using a siRNA-based method. The depletion efficiency of RRM2 was confirmed by western blot analysis (Figure 5A). We chose siRRM2-2# and 3# with better depletion efficiency for additional functional studies. It was observed that depletion of RRM2 significantly inhibits the proliferation of Sk-Mel-2/28 cells by CCK8 and EDU staining (Figures 5B–5E). Moreover, depletion of RRM2 reduces the number of invaded cells and retards the wound closure of melanoma cells (Figures 5F–5I). Our findings demonstrated that RRM2 knockdown greatly reduces the proliferation, invasion, and migration in melanoma cells, same as regorafenib does.

RRM2 overexpression partially reverses regorafenib-induced growth, invasion, and migration suppression of melanoma cells

To examine whether and how RRM2 is involved in regorafenib-induced proliferation inhibition of melanoma cells, RRM2 overexpression plasmid (Figure S3) was transfected into Sk-Mel-2/28 cells and then cells were treated with regorafenib for another 48 h. CCK8 cytotoxicity test showed that RRM2 overexpression partially inhibits regorafenib-induced cytotoxicity of melanoma cells (Figure 6A). Moreover, FCM analysis indicated that RRM2 overexpression appears to partially inhibit the apoptosis induced by regorafenib in melanoma cells (Figures 6B and 6C). In addition, we also observed that RRM2 overexpression partially reverses the suppression of invasion and migration induced by regorafenib in melanoma cells (Figures 6D and 6E). These data suggested regorafenib inhibits the growth, invasion, migration but prompts the apoptosis of melanoma cells through reducing RRM2 expression.

ERK/E2F3 signaling participates the inhibition of regorafenib on melanoma cells

Our RNA-seq data indicated that the downregulated genes induced by regorafenib were enriched in MAPK signaling pathway (Figure 4E). Hence, when melanoma cells were exposed to the appropriate amounts of regorafenib, we attempted to assess the expression of the ERK signaling pathway, the classical MAPK signaling pathway. Western blot analysis revealed that regorafenib treatment reduces the expression of phosphorylated ERK (p-ERK) in melanoma cells (Figure 7A). Importantly, we discovered that E2F3, the downstream transcription factor of ERK signaling, is also one of the 25 ODEGs (Table S2). Consequently, E2F3 expression was also evaluated. When Sk-Mel-2/28 cell lines were given dose-dependent regorafenib treatment, it was observed that E2F3 level likewise decreases (Figure 7A). The above results showed that ERK/E2F3 signaling participates the inhibition of regorafenib on melanoma cells. To investigate how ERK/E2F3 signaling contributes to the inhibition of regorafenib on melanoma cells, Sk-Mel-2/28 cells were treated with specific MEK inhibitor (PD0325901 and U0126) or siRNA-E2F3 to limit ERK signaling or E2F3 expression. Western blot analysis revealed that when ERK signaling is blocked, p-ERK, E2F3, and RRM2 levels are decreased (Figure 7B). Moreover, we noticed that when E2F3 expression is depleted, RRM2 expression is also decreased, which indicated that RRM2 is a downstream molecule of E2F3 (Figure 7C). Our data demonstrated that regorafenib inhibits the pathogenesis of melanoma via ERK/E2F3/RRM2 axis.

Regorafenib reduces tumorigenesis *in vivo*

To prove this hypothesis, tumor allograft was established using SK-Mel-28 and SK-Mel-28 with RRM2 overexpression (we called SK-Mel-28-RRM2), and treatment experiments were performed. Nude mice were first subcutaneously injected with melanoma cells, and once the tumor has formed, the animals were given solvent and 10 mg/kg regorafenib intragastrically every two days. *In vivo* experimental layout was shown in Figure S4A. Our results showed that regorafenib inhibits the growth of xenograft tumors (Figures 8A–8C). To enhance the credibility of *in vivo* experiments, an additional tumor xenograft model using another melanoma cell line SK-Mel-2 was added, and same results were obtained (Figures S4B and S4D). Furthermore, western blot analysis of xenograft tumors indicated that regorafenib treatment inhibited the levels of p-ERK and RRM2, while RRM2 overexpression partially relieved the inhibition of p-ERK and RRM2 expression (Figure 8D), which further validated the results of *in vitro* experiments.

To examine the host toxicity of regorafenib, the vital organs, such as heart, liver, spleen, lung, and kidneys, were harvested from mice and weighed for further histologic examinations. There are no noticeable variations in the weight of these vital organs between control and regorafenib-treatment group (Figure 8E). Moreover, no visible histological alterations in these crucial organs are observed between control and

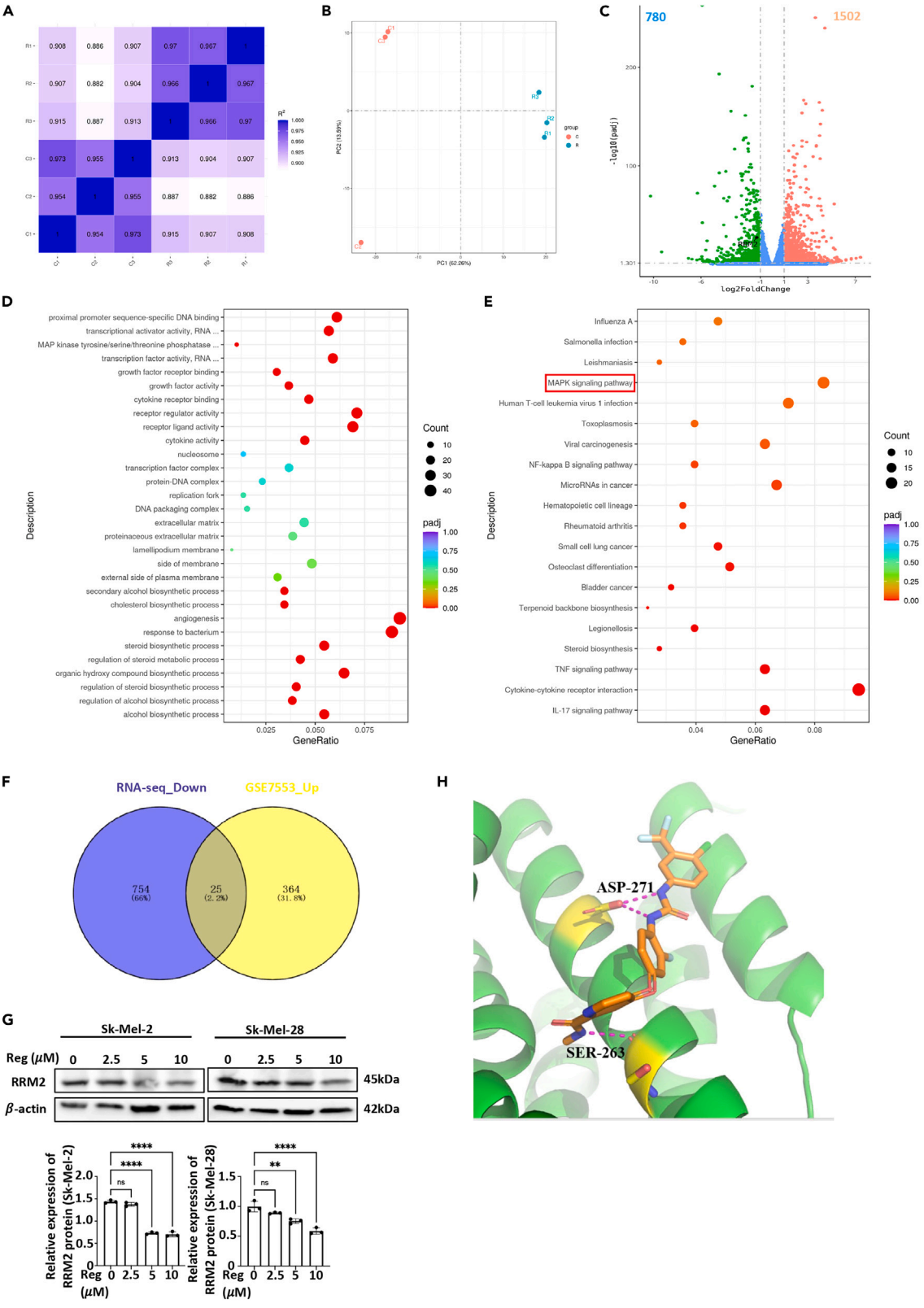
A
B
C
780
1502
D
E
Count
padj
GeneRatio
Description
MAPK signaling pathway
F
RNA-seq_Down
GSE7553_Up
754
(66%)
25
(2.2%)
364
(31.8%)
G
Sk-Mel-2
Sk-Mel-28
Reg (μM) 0 2.5 5 10 0 2.5 5 10
RRM2
β-actin
45kDa
42kDa
Relative expression of RRM2 protein (Sk-Mel-2)
Relative expression of RRM2 protein (Sk-Mel-28)
H
ASP-271
SER-263

Figure 4. RRM2 was the downstream target of regorafenib

(A and B) PCA suggested a clear distinction between regorafenib treatment and control samples.

(C) 1502 upregulated and 780 downregulated DEGs were identified in regorafenib treatment samples by RNA-seq.

(D and E) Downregulated DEGs were used for enrichment analysis.

(F) 25 ODEGs were identified through combining analysis of our RNA-seq_down genes and GSE7553_up genes.

(G) The levels of RRM2 protein were suppressed when melanoma cells were treated with different concentrations of regorafenib.

(H) The predicted binding mode of regorafenib to RRM2 by docking analysis. Reg: regorafenib. $^{**}p < 0.01$, $^{***}p < 0.001$, $^{****}p < 0.0001$. Data are represented as mean ± SEM. Similar results were obtained in two additional independent experiments.

regorafenib-treatment group (Figure S4E), which confirmed that regorafenib has no apparent host toxicity at the effective doses. These data proved that regorafenib has the potential to reduce tumorigenesis *in vivo*.

DISCUSSION

Notwithstanding our huge efforts to treat melanoma,[4,24–26] the overall survival and prognosis of patients have not yet improved. Since melanoma is a highly vascularized, exceedingly malignant malignancy, inhibiting angiogenesis may be a viable treatment strategy.[5] Regorafenib operates as a small-molecule inhibitor of multiple protein kinases,[12] including VEGFR1/2/3 and PDGFR-β, and may become a potential medication in the treatment of melanoma in the future. However, the putative mechanism of regorafenib in melanoma is not fully elucidated, which is the theoretical underpinning for the clinical translational application. Several clinical studies have indicated that regorafenib appears to show extensive anticancer activity in various solid tumors, such as colorectal cancer and GIST.[12,13] Consistent with the studies on regorafenib in solid tumors, our current investigation demonstrated that the anticancer effects of regorafenib are shown in melanoma *in vitro* and *in vivo*.

In our study, we observed that regorafenib dramatically reduces cell proliferation and induces cell death in human melanoma cells *in vitro*. CCK8 cytotoxicity test suggested that regorafenib does exert cytotoxicity on melanoma cells in dose-dependent manner; however, regorafenib does not manifest noticeable cytotoxicity on normal human skin cell lines HEM and Hacat. These results validated regorafenib's safety at an efficacious dosage. Consistently, the inhibition of growth on melanoma cells was confirmed by EdU assay and clone formation assay. Mechanically, regorafenib prevents melanoma cells from growing by blocking the G1 to S cell cycle transition. Moreover, regorafenib induces the apoptosis of melanoma cells by increasing cleaved-PARP and Bax levels while decreasing Bcl-2 level. Due to the metastatic predisposition of melanoma, we also examined the invasion and migration of melanoma cells when treated with regorafenib. Our results indicated that regorafenib inhibits cell invasion and migration in a dose-dependent manner. Excitingly, a phase II clinical study published in 2023 showed that regorafenib therapy demonstrated significant activity in patients with metastatic melanoma harboring c-KIT mutations, with an overall response rate of 30.4% and disease control rate of 73.9%. Adverse events were generally manageable according to the standard guidelines and dose modifications. Their data established that regorafenib should be considered as a treatment option for selected melanoma patients.[27] This clinical study also increased our confidence in future research on regorafenib and melanoma.

Next, we sought to explore the probable mechanism of regorafenib's effects on melanoma growth inhibition. RNA-seq technology and western blot analysis help determine that RRM2 is the downstream target of regorafenib. RRM2, a ribonucleotide reductase component, could synthesize deoxyribonucleotides which is required for DNA repair and replication.[17] RRM2 expression is elevated in the majority of malignancies and thought to be an oncogenic protein.[14,28–31] Related studies showed that RRM2 is a target of ubiquitin specific processing protease (USP) 7 and is regulated by USP7 during S phase of the cell cycle. Genetic and pharmacological inhibition of USP7 induces senescence in melanoma cells. The therapeutic combination of bifunctional histone deacetylase (HDAC)/LSD1 inhibitor domatinostat and USP7 inhibitor P5091 benefits individuals with melanoma.[22] Moreover, RRM2 is considered to be a novel target of sorafenib, partially contributing to its anticancer activity in hepatocellular carcinoma (HCC) cells.[32] Similarly, our results demonstrated that RRM2 acts as a target of regorafenib to participate in the growth inhibition by regorafenib in melanoma.

In addition, our RNA-seq data showed that the downregulated DEGs are enriched in MAPK signaling pathway. And we examined the expression of ERK signaling, the classical MAPK pathway, when different doses of regorafenib were administered. Our results indicated that regorafenib treatment prevents ERK phosphorylation in melanoma cells. In addition, we also measured the level of E2F3, downstream molecule of ERK signaling. E2F3 and RRM2 are the downregulated genes in regorafenib-treatment group, and also the upregulated genes in melanoma datasets Database: GSE7553. This hinted us that regorafenib may reduce RRM2 expression by inhibiting E2F3 activity. As we predicted, when melanoma cells are treated with certain quantities of regorafenib, both of E2F3 and RRM2 levels are decreased. Moreover, when E2F3 expression is depleted using siRNA technology, RRM2 level is reduced, which indicated that RRM2 is the downstream target of E2F3. It has been proven that E2F3 promotes cancer cell growth and is overexpressed in human melanoma,[33,34] but the study is limited. Our study deepens understanding of E2F3's role in melanoma etiology.

In conclusion, our findings concluded that regorafenib inhibits melanoma cell proliferation, invasion, and migration while inducing apoptosis through the ERK/E2F3/RRM2 axis. Our study showed that regorafenib may prove to be a promising therapeutic agent for melanoma.

Limitations of the study

In our study, we only examined ERK signaling (the classical type of MAPK signaling) in the inhibition induced by regorafenib in melanoma cells, other MAPK signaling pathways (JNK, p38, and ERK5 signaling) were not yet examined.

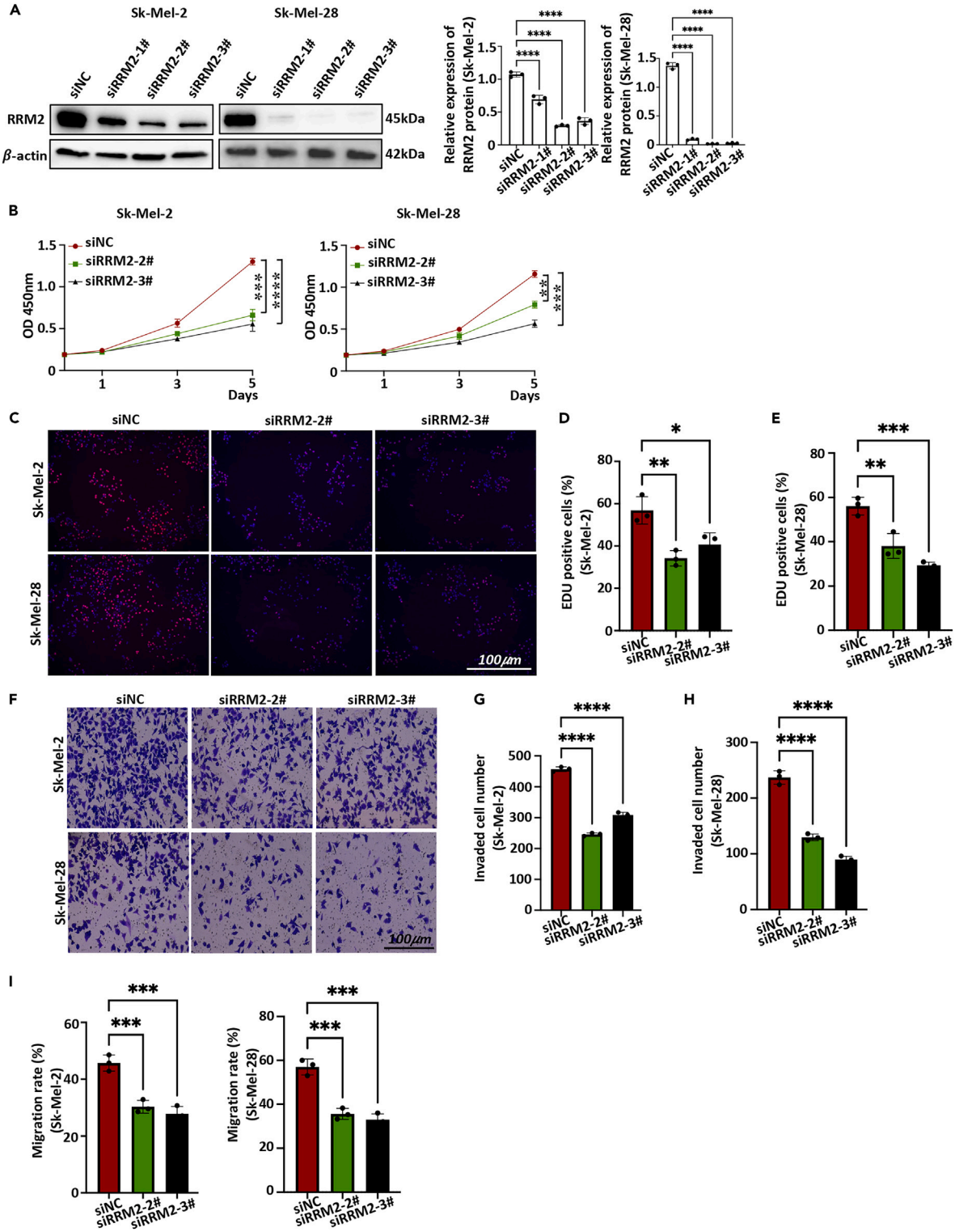

Figure 5. Depletion of RRM2 alleviated the malignancy of melanoma cells

(A) The depletion efficiency of RRM2 was confirmed by western blot analysis.

(B–E) Depletion of RRM2 significantly inhibited the proliferation of Sk-Mel-2/28 cells by CCK8 (B) and EDU staining (C–E).

(F–I) RRM2 depletion reduced the number of invaded cells (F–H) and retarded the wound closure of melanoma cells (I). *$p < 0.05$, **$p < 0.01$, ***$p < 0.001$, ****$p < 0.0001$. Data are represented as mean ± SEM. Similar results were obtained in two additional independent experiments. (C + F) Scale bar: 100 μm.

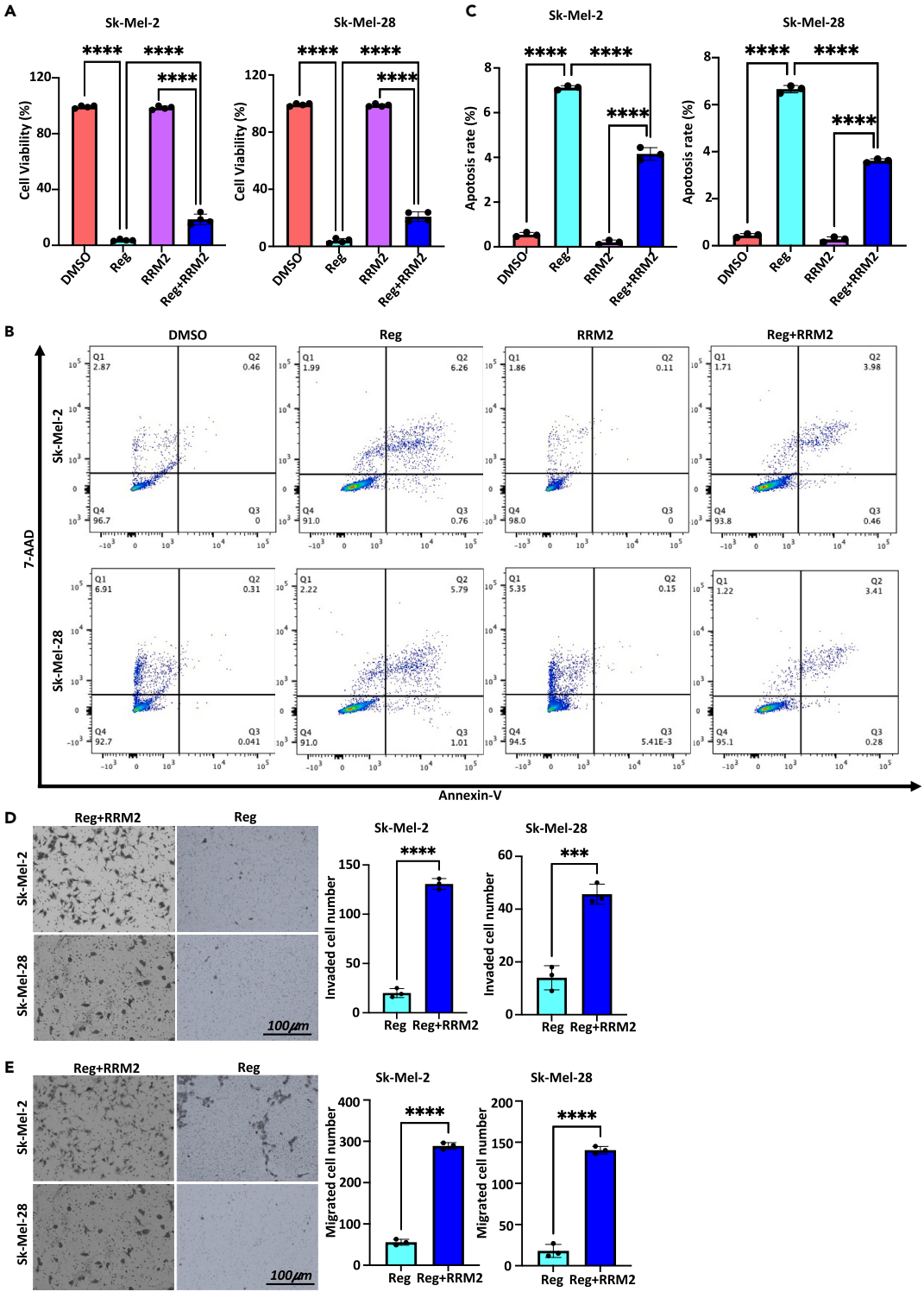

Figure 6. RRM2 overexpression partially reversed regorafenib-induced growth inhibition of melanoma cells

(A) RRM2 overexpression partially reversed regorafenib-induced cytotoxicity of melanoma cells by CCK8 cytotoxicity test.

(B and C) RRM2 overexpression partially reduced regorafenib-induced apoptosis of melanoma cells by FCM.

(D and E) RRM2 overexpression partially reverses the suppression of invasion and migration induced by regorafenib in melanoma cells by transell assays. Scale bar: 100 μm. Reg: regorafenib. ***$p < 0.001$, ****$p < 0.0001$. Data are represented as mean ± SEM. Similar results were obtained in two additional independent experiments.

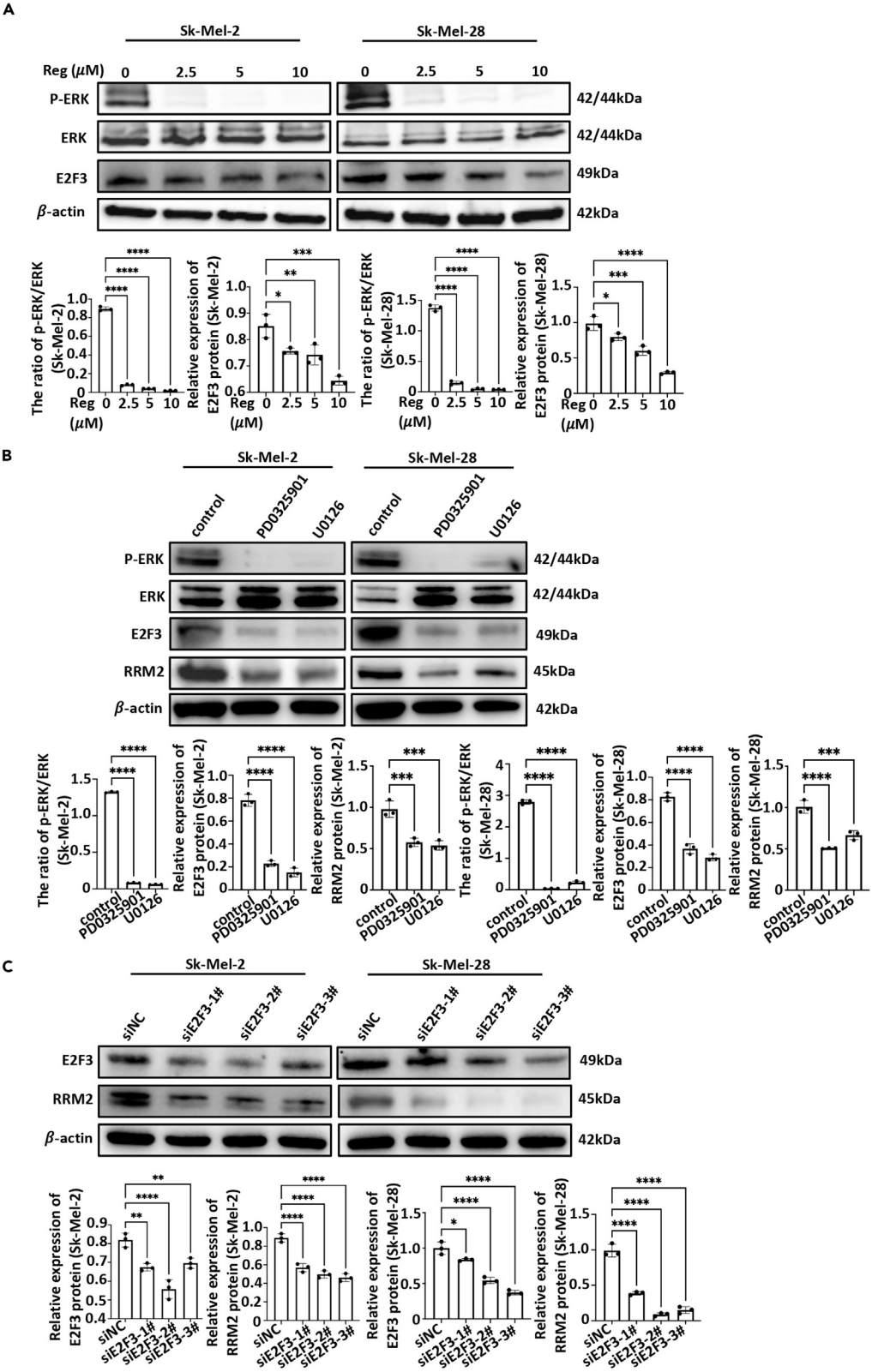
A
Sk-Mel-2
Sk-Mel-28
Reg (μM) 0 2.5 5 10 0 2.5 5 10
P-ERK
ERK
E2F3
β-actin
42/44kDa
42/44kDa
49kDa
42kDa
The ratio of p-ERK/ERK (Sk-Mel-2)
Relative expression of E2F3 protein (Sk-Mel-2)
The ratio of p-ERK/ERK (Sk-Mel-28)
Relative expression of E2F3 protein (Sk-Mel-28)
Reg (μM) 0 2.5 5 10
B
Sk-Mel-2
Sk-Mel-28
control
PD0325901
U0126
P-ERK
ERK
E2F3
RRM2
β-actin
42/44kDa
42/44kDa
49kDa
45kDa
42kDa
The ratio of p-ERK/ERK (Sk-Mel-2)
Relative expression of E2F3 protein (Sk-Mel-2)
Relative expression of RRM2 protein (Sk-Mel-2)
The ratio of p-ERK/ERK (Sk-Mel-28)
Relative expression of E2F3 protein (Sk-Mel-28)
Relative expression of RRM2 protein (Sk-Mel-28)
C
Sk-Mel-2
Sk-Mel-28
siNC
siE2F3-1#
siE2F3-2#
siE2F3-3#
E2F3
RRM2
β-actin
49kDa
45kDa
42kDa
Relative expression of E2F3 protein (Sk-Mel-2)
Relative expression of RRM2 protein (Sk-Mel-2)
Relative expression of E2F3 protein (Sk-Mel-28)
Relative expression of RRM2 protein (Sk-Mel-28)

Figure 7. ERK/E2F3 signaling participated the inhibition of regorafenib on melanoma cells

(A) The expression of p-ERK and E2F3 were inhibited when melanoma cells were treated with regorafenib by western blot.

(B) When ERK signaling was blocked, the level of p-ERK, E2F3, and RRM2 was reduced.

(C) When E2F3 expression was depleted, RRM2 expression was also depleted. Reg: regorafenib. *$p < 0.05$, **$p < 0.01$, ***$p < 0.001$, ****$p < 0.0001$. Data are represented as mean ± SEM. Similar results were obtained in two additional independent experiments.

RESOURCE AVAILABILITY

Lead contact

Further information and requests for resources and reagents should be directed to and will be fulfilled by the lead contact, Xiuyun Xuan (xiuyunxuanlw@163.com).

Materials availability

This study did not generate any new lines.

This study did not generate new, unique reagents.

Data and code availability

- RNA-seq data are publicly accessible through NCBI using accession number Database: GSE273844.
- This paper does not report original code.
- Any additional information required to reanalyze the data reported in this paper is available from the lead contact upon request.

ACKNOWLEDGMENTS

This work was supported by grants from the General Program of the National Natural Science Foundation of China (no. 81972565).

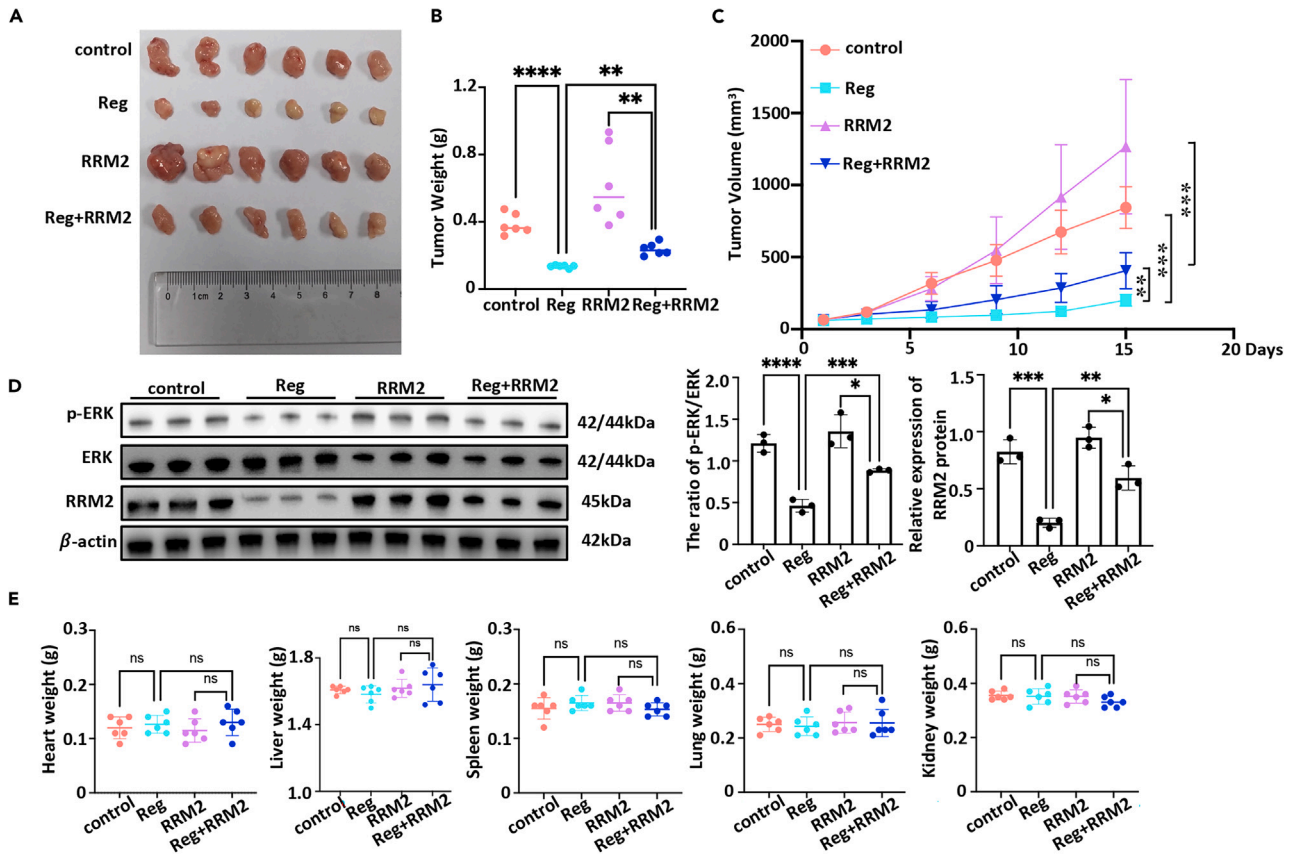

Figure 8. Regorafenib reduced tumorigenesis *in vivo*

(A–C) Regorafenib inhibited the growth of xenograft tumors, including tumor weight (B) and volume (C).

(D) Regorafenib treatment inhibited the levels of p-ERK and RRM2, while RRM2 overexpression partially relieved the inhibition of p-ERK and RRM2 expression.

(E) There were no obvious differences in the weight of these vital organs between control and regorafenib-treatment group. **$p < 0.01$, ***$p < 0.001$, ****$p < 0.0001$. Data are represented as mean ± SEM. Similar results were obtained in two additional independent experiments.

AUTHOR CONTRIBUTIONS

X.X. composed the manuscript and drew the figures. Y.L., C.H., and Y.Z. edited the manuscript. All authors read and approved the final manuscript.

DECLARATION OF INTERESTS

The authors declare no competing interests.

STAR★METHODS

Detailed methods are provided in the online version of this paper and include the following:

- KEY RESOURCES TABLE
- EXPERIMENTAL MODEL AND STUDY PARTICIPANT DETAILS
  - Ethical approval
  - Cell lines
  - Melanoma mouse model
- METHOD DETAILS
  - Drug preparation
  - CCK8 cytotoxicity test
  - EdU assay
  - Cell colony formation assay
  - Wound healing assay
  - Transwell assays
  - Flow cytometry (FCM)
  - Immunofluorescence staining
  - Quantified real-time PCR (qRT-PCR)
  - Western blot analysis
  - HE staining
  - Cell transfection
  - RNA-sequencing (RNA-seq) and data analysis
  - Molecular docking
- QUANTIFICATION AND STATISTICAL ANALYSIS

SUPPLEMENTAL INFORMATION

Supplemental information can be found online at https://doi.org/10.1016/j.isci.2024.110993.

Received: March 14, 2024
Revised: July 30, 2024
Accepted: September 16, 2024
Published: September 19, 2024

REFERENCES

1. Carr, S., Smith, C., and Wernberg, J. (2020). Epidemiology and Risk Factors of Melanoma. Surg. Clin. *100*, 1–12. https://doi.org/10.1016/j.suc.2019.09.005.
2. Davis, L.E., Shalin, S.C., and Tackett, A.J. (2019). Current state of melanoma diagnosis and treatment. Cancer Biol. Ther. *20*, 1366–1379. https://doi.org/10.1080/15384047.2019.1640032.
3. Zeng, H., Li, J., Hou, K., Wu, Y., Chen, H., and Ning, Z. (2022). Melanoma and Nanotechnology-Based Treatment. Front. Oncol. *12*, 858185. https://doi.org/10.3389/fonc.2022.858185.
4. Swetter, S.M., Tsao, H., Bichakjian, C.K., Curiel-Lewandrowski, C., Elder, D.E., Gershenwald, J.E., Guild, V., Grant-Kels, J.M., Halpern, A.C., Johnson, T.M., et al. (2019). Guidelines of care for the management of primary cutaneous melanoma. J. Am. Acad. Dermatol. *80*, 208–250. https://doi.org/10.1016/j.jaad.2018.08.055.
5. Castet, F., Garcia-Mulero, S., Sanz-Pamplona, R., Cuellar, A., Casanovas, O., Caminal, J.M., and Piulats, J.M. (2019). Uveal Melanoma, Angiogenesis and Immunotherapy, Is There Any Hope? Cancers *11*, 834. https://doi.org/10.3390/cancers11060834.
6. Ferrara, N., Gerber, H.P., and LeCouter, J. (2003). The biology of VEGF and its receptors. Nat. Med. *9*, 669–676. https://doi.org/10.1038/nm0603-669.
7. Chen, Y., Zhang, L., Liu, W.X., and Wang, K. (2018). VEGF and SEMA4D have synergistic effects on the promotion of angiogenesis in epithelial ovarian cancer. Cell. Mol. Biol. Lett. *23*, 2. https://doi.org/10.1186/s11658-017-0058-9.
8. Zhou, Y., Zhu, X., Cui, H., Shi, J., Yuan, G., Shi, S., and Hu, Y. (2021). The Role of the VEGF Family in Coronary Heart Disease. Front. Cardiovasc. Med. *8*, 738325. https://doi.org/10.3389/fcvm.2021.738325.
9. Wilhelm, S.M., Dumas, J., Adnane, L., Lynch, M., Carter, C.A., Schütz, G., Thierauch, K.H., and Zopf, D. (2011). Regorafenib (BAY 73-4506): a new oral multikinase inhibitor of angiogenic, stromal and oncogenic receptor tyrosine kinases with potent preclinical antitumor activity. Int. J. Cancer *129*, 245–255. https://doi.org/10.1002/ijc.25864.
10. Davis, S.L., Eckhardt, S.G., Messersmith, W.A., and Jimeno, A. (2013). The development of regorafenib and its current and potential future role in cancer therapy. Drugs Today *49*, 105–115. https://doi.org/10.1358/dot.2013.49.2.1930525.
11. Chen, D., Wei, L., Yu, J., and Zhang, L. (2014). Regorafenib inhibits colorectal tumor growth through PUMA-mediated apoptosis. Clin. Cancer Res. *20*, 3472–3484. https://doi.org/10.1158/1078-0432.CCR-13-2944.
12. Grothey, A., Van Cutsem, E., Sobrero, A., Siena, S., Falcone, A., Ychou, M., Humblet, Y., Bouché, O., Mineur, L., Barone, C., et al. (2013). Regorafenib monotherapy for previously treated metastatic colorectal cancer (CORRECT): an international, multicentre, randomised, placebo-controlled, phase 3 trial. Lancet *381*, 303–312. https://doi.org/10.1016/S0140-6736(12)61900-X.
13. Li, J., Qin, S., Xu, R., Yau, T.C.C., Ma, B., Pan, H., Xu, J., Bai, Y., Chi, Y., Wang, L., et al. (2015). Regorafenib plus best supportive care versus placebo plus best supportive care in Asian patients with previously treated metastatic colorectal cancer (CONCUR): a randomised, double-blind, placebo-controlled, phase 3 trial. Lancet Oncol. *16*, 619–629. https://doi.org/10.1016/S1470-2045(15)70156-7.
14. Yang, Y., Lin, J., Guo, S., Xue, X., Wang, Y., Qiu, S., Cui, J., Ma, L., Zhang, X., and Wang, J. (2020). RRM2 protects against ferroptosis and is a tumor biomarker for liver cancer. Cancer

Cell Int. *20*, 587. https://doi.org/10.1186/s12935-020-01689-8.
15. Lin, Z.P., Belcourt, M.F., Cory, J.G., and Sartorelli, A.C. (2004). Stable suppression of the R2 subunit of ribonucleotide reductase by R2-targeted short interference RNA sensitizes p53(-/-) HCT-116 colon cancer cells to DNA-damaging agents and ribonucleotide reductase inhibitors. J. Biol. Chem. *279*, 27030–27038. https://doi.org/10.1074/jbc.M402056200.
16. Gandhi, M., Groß, M., Holler, J.M., Coggins, S.A., Patil, N., Leupold, J.H., Munschauer, M., Schenone, M., Hartigan, C.R., Allgayer, H., et al. (2020). The lncRNA lincNMR regulates nucleotide metabolism via a YBX1 - RRM2 axis in cancer. Nat. Commun. *11*, 3214. https://doi.org/10.1038/s41467-020-17007-9.
17. Mazzu, Y.Z., Armenia, J., Chakraborty, G., Yoshikawa, Y., Coggins, S.A., Nandakumar, S., Gerke, T.A., Pomerantz, M.M., Qiu, X., Zhao, H., et al. (2019). A Novel Mechanism Driving Poor-Prognosis Prostate Cancer: Overexpression of the DNA Repair Gene, Ribonucleotide Reductase Small Subunit M2 (RRM2). Clin. Cancer Res. *25*, 4480–4492. https://doi.org/10.1158/1078-0432.CCR-18-4046.
18. Rasmussen, R.D., Gajjar, M.K., Tuckova, L., Jensen, K.E., Maya-Mendoza, A., Holst, C.B., Møllgaard, K., Rasmussen, J.S., Brennum, J., Bartek, J., Jr., et al. (2016). BRCA1-regulated RRM2 expression protects glioblastoma cells from endogenous replication stress and promotes tumorigenicity. Nat. Commun. *7*, 13398. https://doi.org/10.1038/ncomms13398.
19. Duxbury, M.S., and Whang, E.E. (2007). RRM2 induces NF-kappaB-dependent MMP-9 activation and enhances cellular invasiveness. Biochem. Biophys. Res. Commun. *354*, 190–196. https://doi.org/10.1016/j.bbrc.2006.12.177.
20. Morikawa, T., Maeda, D., Kume, H., Homma, Y., and Fukayama, M. (2010). Ribonucleotide reductase M2 subunit is a novel diagnostic marker and a potential therapeutic target in bladder cancer. Histopathology *57*, 885–892. https://doi.org/10.1111/j.1365-2559.2010.03725.x.
21. Souglakos, J., Boukovinas, I., Taron, M., Mendez, P., Mavroudis, D., Tripaki, M., Hatzidaki, D., Koutsopoulos, A., Stathopoulos, E., Georgoulias, V., and Rosell, R. (2008). Ribonucleotide reductase subunits M1 and M2 mRNA expression levels and clinical outcome of lung adenocarcinoma patients treated with docetaxel/gemcitabine. Br. J. Cancer *98*, 1710–1715. https://doi.org/10.1038/sj.bjc.6604344.
22. Granieri, L., Marocchi, F., Melixetian, M., Mohammadi, N., Nicoli, P., Cuomo, A., Bonaldi, T., Confalonieri, S., Pisati, F., Giardina, G., et al. (2022). Targeting the USP7/RRM2 axis drives senescence and sensitizes melanoma cells to HDAC/LSD1 inhibitors. Cell Rep. *40*, 111396. https://doi.org/10.1016/j.celrep.2022.111396.
23. Fatkhutdinov, N., Sproesser, K., Krepler, C., Liu, Q., Brafford, P.A., Herlyn, M., Aird, K.M., and Zhang, R. (2016). Targeting RRM2 and Mutant BRAF Is a Novel Combinatorial Strategy for Melanoma. Mol. Cancer Res. *14*, 767–775. https://doi.org/10.1158/1541-7786.MCR-16-0099.
24. Dhillon, S. (2022). Tebentafusp: First Approval. Drugs *82*, 703–710. https://doi.org/10.1007/s40265-022-01704-4.
25. Rigel, D.S., and Carucci, J.A. (2000). Malignant melanoma: prevention, early detection, and treatment in the 21st century. CA Cancer J. Clin. *50*, 215–240. https://doi.org/10.3322/canjclin.50.4.215.
26. Lo, J.A., and Fisher, D.E. (2014). The melanoma revolution: from UV carcinogenesis to a new era in therapeutics. Science *346*, 945–949. https://doi.org/10.1126/science.1253735.
27. Kim, K.H., Jung, M., Lee, H.J., Lee, S.J., Kim, M., Ahn, M.S., Choi, M.Y., Lee, N.R., and Shin, S.J.; Korean Cancer Study Group KCSG (2023). A phase II study on the efficacy of regorafenib in treating patients with c-KIT-mutated metastatic malignant melanoma that progressed after previous treatment (KCSG-UN-14-13). Eur. J. Cancer *193*, 113312. https://doi.org/10.1016/j.ejca.2023.113312.
28. Xiong, W., Zhang, B., Yu, H., Zhu, L., Yi, L., and Jin, X. (2021). RRM2 Regulates Sensitivity to Sunitinib and PD-1 Blockade in Renal Cancer by Stabilizing ANXA1 and Activating the AKT Pathway. Adv. Sci. *8*, e2100881. https://doi.org/10.1002/advs.202100881.
29. Jin, C.Y., Du, L., Nuerlan, A.H., Wang, X.L., Yang, Y.W., and Guo, R. (2020). High expression of RRM2 as an independent predictive factor of poor prognosis in patients with lung adenocarcinoma. Aging (Albany NY) *13*, 3518–3535. https://doi.org/10.18632/aging.202292.
30. Zhan, Y., Jiang, L., Jin, X., Ying, S., Wu, Z., Wang, L., Yu, W., Tong, J., Zhang, L., Lou, Y., and Qiu, Y. (2021). Inhibiting RRM2 to enhance the anticancer activity of chemotherapy. Biomed. Pharmacother. *133*, 110996. https://doi.org/10.1016/j.biopha.2020.110996.
31. Pfister, S.X., Markkanen, E., Jiang, Y., Sarkar, S., Woodcock, M., Orlando, G., Mavrommati, I., Pai, C.C., Zalmas, L.P., Drobnitzky, N., et al. (2015). Inhibiting WEE1 Selectively Kills Histone H3K36me3-Deficient Cancers by dNTP Starvation. Cancer Cell *28*, 557–568. https://doi.org/10.1016/j.ccell.2015.09.015.
32. Yang, P.M., Lin, L.S., and Liu, T.P. (2020). Sorafenib Inhibits Ribonucleotide Reductase Regulatory Subunit M2 (RRM2) in Hepatocellular Carcinoma Cells. Biomolecules *10*, 117. https://doi.org/10.3390/biom10010117.
33. Feng, Z., Peng, C., Li, D., Zhang, D., Li, X., Cui, F., Chen, Y., and He, Q. (2018). E2F3 promotes cancer growth and is overexpressed through copy number variation in human melanoma. OncoTargets Ther. *11*, 5303–5313. https://doi.org/10.2147/OTT.S174103.
34. Xia, Y., Zhou, Y., Han, H., Li, P., Wei, W., and Lin, N. (2019). lncRNA NEAT1 facilitates melanoma cell proliferation, migration, and invasion via regulating miR-495-3p and E2F3. J. Cell. Physiol. *234*, 19592–19601. https://doi.org/10.1002/jcp.28559.
35. Xuan, X., Zhou, J., Tian, Z., Lin, Y., Song, J., Ruan, Z., Ni, B., Zhao, H., and Yang, W. (2020). ILC3 cells promote the proliferation and invasion of pancreatic cancer cells through IL-22/AKT signaling. Clin. Transl. Oncol. *22*, 563–575. https://doi.org/10.1007/s12094-019-02160-5.

STAR★METHODS

KEY RESOURCES TABLE

REAGENT or RESOURCE	SOURCE	IDENTIFIER
Antibodies		
PARP/cleaved PARP	Zenbio	380374
Bcl-2	Proteintech	12789-1-AP; RRID: AB_2227948
Bax	Bioswamp	PAB46088
PARP/cleaved-PARP	Proteintech	13371-1-AP; RRID: AB_2160459
Bax	Proteintech	50599-2-Ig; RRID: AB_2061561
phospho-p44/42 MAPK (Erk1/2)	Cell Signaling Technology	4370; RRID: AB_2315112
p44/42 MAPK (Erk1/2)	Cell Signaling Technology	4695; RRID: AB_390779
RRM2	Bimake	A5504
E2F3	Affinity Biosciences	DF12390; RRID: AB_2845195
β-actin	Proteintech	20536-1-AP; RRID: AB_10700003
Critical commercial assay		
BeyoClick™ EdU-594 Imaging Kits	Beyotime	C0078S
apoptosis detection kit	Multi Science	AP104
cell cycle analysis kit	Yeasen Biotechnology	40301ES60
DAPI	Servicebio	G1012
PrimeScript RT Reagent Kit	Vazyme	R323-01
2x SYBR Green qPCR Master Mix	Bimake	B21202
Deposited data		
Raw and analyzed data	This paper	Database: GSE273844
Experimental models: Cell lines		
A2058	Shanghai Jinyuan Biotechnology	A2058
SK-MEL-2	Shanghai Jinyuan Biotechnology	SK-MEL-2
SK-MEL-28	Shanghai Jinyuan Biotechnology	SK-MEL-28
MUM-2B	Shanghai Jinyuan Biotechnology	MUM-2B
HEM	ATCC cell bank	HEM
Hacat	PriCells	Hacat
Oligonucleotides		
See Table S1 for a list of oligonucleotides		
Software and algorithms		
ImageJ	ImageJ	https://imagej.nih.gov/ij/
Adobe Photoshop	Adobe Photoshop	https://www.adobe.com/es/
Prism	Prism	https://www.graphpad.com/
AutoDockTools 1.5.7	AutoDockTools 1.5.7	https://autodock.scripps.edu/
FlowJo	FlowJo	https://www.flowjo.com/
WPS Office	WPS Office	https://www.wps.cn/

EXPERIMENTAL MODEL AND STUDY PARTICIPANT DETAILS

Ethical approval

The experimental procedures adhered to the guidelines outlined in the National Institutes of Health Guide for the Care and Use of Laboratory Animals. Ethical approval for this study was obtained from the Institutional Animal Care and Use Committee (IACUC) of Tongji Medical college, Huazhong science and technology (IACUC number is 3287).

Cell lines

Human melanoma cells (A2058, SK-MEL-2, SK-MEL-28 and MUM-2B) were purchased from Shanghai Jinyuan Biotechnology (Shanghai, China). A2058 was grown in DMEM medium (Gibco, USA) supplemented with 10% fetal bovine serum (FBS, #10270-106, Gibco, USA), while SK-MEL-2, SK-MEL-28 and MUM-2B were grown in RPMI-1640 medium (Gibco, USA) supplemented with 10% FBS. Normal human skin cells (HEM and Hacat) were provided from ATCC cell bank and PriCells (wuhan, China), respectively. HEM was grown in RPMI-1640 medium (Gibco, USA) supplemented with 10% FBS, while Hacat was grown in DMEM medium (Gibco, USA) supplemented with 10% FBS.

Melanoma mouse model

BALB/c nude mice, female, 4–6 weeks old, were kept in the SPF barrier facilities of Tongji Medical college, Huazhong science and technology. SK-Mel-2/28 cells (10^7 cells, 100 uL) were injected subcutaneously into their right waists. About ten days, mice were divided into three groups randomly, which were treated every two days with vehicle or 10 mg/kg of regorafenib intragastrically. Tumor size and volume were measured every 3 days, and tumor volume was calculated according to the formula: volume (mm^3) = (0.523) × length (mm) × width (mm) × height (mm). Mice were sacrificed when xenograft tumors in control group reached about 1 cm^3, and xenograft tumor tissues and important organs were removed, photographed, weighted, and preserved for further investigation.

METHOD DETAILS

Drug preparation

Regorafenib (#755037-03-7, ApexBio, USA) was dissolved in dimethyl sulfoxide (DMSO) with a stock concentration of 10 mM and stored at −20°C. For *in vitro* study, regorafenib with different concentrations (0, 2.5, 5, 10 μM) were used for different experiments.

CCK8 cytotoxicity test

The effects of regorafenib's cytotoxicity on melanoma cells or normal human skin cells were assessed by CCK8 assay. Briefly, cells (5000 cells/well) were seeded in 96-well plates, regorafenib treatment with different concentrations (0, 2.5, 5, 10 μM) began after 12 h. Cells were cultured in the presence of regorafenib for 24h or 48h. At the end of each culture period, 10 μL of the CCK-8 solution (ApexBio, USA) was added to each well. After 1.5 h of incubation, the absorbance at 450 nm was examined. Three independent assays were repeated.

EdU assay

The EdU assay was conducted using BeyoClick EdU-594 Imaging Kits (C0078S, Beyotime, China) according to the manufacturer's protocol. Briefly, 1000 SK-MEL-2/28 cells were seeded into the 6-well plates, and incubated with regorafenib (0, 2.5, 5, 10 μM) for 48 h. After incubation of 10 μM EdU for 2 h, cells were fixed with 4% paraformaldehyde for 15 min and permeabilized with Triton X-100 for 20 min. Then, the incorporated EdU was visualized by means of a click reaction for 30 min and the nuclear DNA was stained with Hoechst 33342 for 30 min. Finally, the proliferative cells were observed using a fluorescence microscope and the percentage of EdU-positive cells were assessed using the ImageJ software. Three independent assays were repeated.

Cell colony formation assay

100 cells of SK-MEL-2 and SK-MEL-28 cells were seeded into 6-well plate. Cells were treated with indicated concentrations of regorafenib, and the medium was refreshed every 3 days. After culturing for 2 weeks or when the number of cells in most single clones was more than 50, the colony formation ended. The colonies were fixed with 4% paraformaldehyde and dyed with crustal violet for 15 min. Colonies were photographed using a microscope and a digital camera, and the numbers of colonies were counted via ImageJ software. Three independent assays were repeated.

Wound healing assay

The procedure was conducted as described.[35] 5×10^5 SK-MEL-2/28 cells were seeded in 6-well plates for adherent culture and a sterile 200-μL pipette tip was used to make the scratches. The wounded cells were then treated with indicated concentrations of regorafenib after removing debris by PBS for 24 and 48 h. The scratch area was captured at 0, 24 and 48 h, and the migration rate were measured by ImageJ. Three independent assays were repeated.

Transwell assays

SK-MEL-2 and SK-MEL-28 cells were treated with indicated concentrations of regorafenib for 48h and were resuspended at different density (5×10^4 cells/well, 200 μL) and seeded in the upper chambers (24-well migration chambers, 8.0 μm pore membrane, Corning, USA) in the serum-free medium. The upper chambers were precoated with Matrigel (Sigma) or not. Then, the lower chambers were filled with 800 μL of the medium with 10% FBS. After 24 h incubation, the non-invasive cells were wiped of the upper sides of the upper chambers with a cotton swab. The lower sides of the upper chambers were fixed with 4% paraformaldehyde and stained with crystal violet. Five fields were randomly selected, and invaded or migrated cells were counted. Three independent assays were repeated.

Flow cytometry (FCM)

For apotosis and cell cycle analysis, regorafenib-treated cells were performed by an apoptosis detection kit (AP104, Multi Science, China) and cell cycle analysis kit (40301ES60, Yeasen Biotechnology, China) following their instructions. Briefly, 5×10^4 melanoma cells were treated with different concentrations of regorafenib for 48h. Then cells were collected and counted, cells were fixed with 4% paraformaldehyde or not, staining solution (staining buffer is 5 ×Binding buffer for AP104 and staining solution [40301-C] for 40301ES60, dye is Annexin V-PE and 7-AAD for AP104, PI for 40301ES60) was prepared, and then cells were incubated in the staining solution for indicated minutes at 37°C at dark. Then, the staining solution was taken away, and stained cells were detected by FCM. The frequency of apoptotic cells and cell cycle distribution were analyzed by FlowJo software. Three independent assays were repeated.

Immunofluorescence staining

SK-MEL-2 and SK-MEL-28 cells (5×10^4 cells/well) were seeded into 6-well plates, and after 12 h, cells were treated with indicated concentrations of regorafenib for another 48h. Then cells were fixed with 4% polyformaldehyde, permeabilized with Triton X-100, blocked with 5% bovine serum, and incubated with anti-cleaved PARP (1:100, 380374, Zenbio, China), anti-Bcl-2 (1:100, 12789-1-AP, Proteintech, USA) and anti-Bax (1:100, PAB46088, Bioswamp, China) for whole night at 4°C. Cells were incubated with FITC-conjugated secondary antibody (1:100, GB22403, Servicebio, China) for 1 h, and then nuclei were stained with DAPI (G1012, Servicebio, China) for 2 min. Finally, the apoptotic cells were observed using a fluorescence microscope, and the number of cells were measured by ImageJ. Three independent assays were repeated.

Quantified real-time PCR (qRT-PCR)

Total RNA was extracted using TRIzol reagent (R401-01, Vazyme, China) and then 1μg RNA was reverse-transcribed to cDNA with a PrimeScript RT Reagent Kit (R323-01, Vazyme, China) according to the manufacturer's instructions. QRT-PCR was carried out on Step One plus real-time PCR system using 2× SYBR Green qPCR Master Mix (B21202, Bimake, USA). The running conditions were 10 min at 95°C, followed by 40 cycles of 15 s at 95°C, 30 s at 60°C and 30 s at 72°C, and then for a melting curve, 15 s at 95°C, 1 min at 60°C, and 15 s at 95°C. Relative expression of each gene was calculated according to the $2^{-\Delta\Delta t}$ method. β-actin was used as an internal control for normalization. The primer sequences were provided in Table S1. Three independent assays were repeated.

Western blot analysis

SK-MEL-2 and SK-MEL-28 cells were treated with indicated concentrations of regorafenib for 48h. And, total proteins of cells were extracted using RIPA buffer supplemented with 1% phosphoproteinase inhibitors (Solarbio, China) on ice, and then quantified by BCA protein assay kit (Beyotime, China). The protein samples (30 μg) were resolved by sodium dodecyl sulfate–polyacrylamide gel electrophoresis (SDS-PAGE) and transferred onto polyvinylidene fluoride (PVDF) membranes for immunoblotting, and then blocked with 5% skimmed milk, and then incubated with the primary antibody overnight at 4°C. The membranes were incubated with horseradish peroxidase (HRP)-conjugated secondary antibodies for 1 h at room temperature and visualized with a chemiluminescent detection system (Pierce ECL Substrate Western Blot Detection System; Thermo Scientifc, Rockford, MA, USA) and exposure to autoradiographic film (Kodak XAR flm). β-actin was used as the loading control. The primary antibodies were as follows: anti-PARP/cleaved-PARP (1:1000, 13371-1-AP, Proteintech, USA), Bax (1:5000, 50599-2-Ig, Proteintech, USA), Bcl-2 (1:5000, 12789-1-AP, Proteintech, USA), anti-phospho-p44/42 MAPK (Erk1/2) (1:1000, 4370, Cell Signaling Technology, USA), anti-p44/42 MAPK (Erk1/2) (1:1000, 4695, Cell Signaling Technology, USA), RRM2 (1:1000, A5504, Bimake, USA), E2F3 (1:1000, DF12390, Affinity Biosciences, USA) and β-actin (1:3000, 20536-1-AP, Proteintech, USA). The second antibodies were as follows: HRP-conjugated Affinipure Goat Anti-Rabbit IgG(H + L) (1:5000, SA00001-2, Proteintech, USA). Three independent assays were repeated.

HE staining

The vital organs of tumor xenograft model were fixed in 4% paraformaldehyde and were embedded in paraffin. 5-μm sections were obtained and stained with hematoxylin and eosin (H&E). The tissue pathology under microscope was observed. Three independent assays were repeated.

Cell transfection

SiRNAs against RRM2 and E2F3, and RRM2 overexpression plasmid were designed and synthesized by TsingkeBiotechnology (China). The siRNAs and plasmid were transfected into SK-Mel-2 and SK-Mel-28 cells using EndoFectinTM Max transfection reagent (EF013, GeneCopoeia) according to the manufacturer's protocols. Western blotting were used for conforming the efficiency of silencing after 72 h of transfection. The target sequences were provided in Table S1. Three independent assays were repeated.

RNA-sequencing (RNA-seq) and data analysis

5×10^4 Sk-Mel-2 cells were treated with regorafenib (DMSO or 10 μM) respectively. After 48 h of treatment, total RNA of Sk-Mel-2 cells were extracted. The cDNA libraries were constructed for each RNA sample using the TruSeq Stranded mRNA Library Prep Kit (Illumina, US) according to the manufacturer's instructions. The mRNA library was prepared from total RNA using the NEB Next Small RNA Library Prep. Before read mapping, clean reads were obtained from the raw reads by removing the adapter sequences and low-quality reads. The clean reads

were then aligned to the human genome (GRCh38, NCBI) using Hisat2. HTseq was used to calculate gene counts, and the RPKM method was used to determine relative gene expression. Differential expression analysis of two conditions/groups was performed using the DESeq2 R package (1.16.1). The resulting *p*-values were adjusted using the Benjamini and Hochberg's approach for controlling the false discovery rate. The $|\log_2 \text{Fold Change}| \geq 1$ with *p*-value <0.05 were set as the cutoff criteria by DESeq2 were defined Differential Expression Genes (DEGs) for further investigation in this study.

Molecular docking

The regorafenib's 3D structural files in SDF format were obtained from the PubChem database and then converted to PDB format using Open Babel. The 3D crystal structure of RRM2 was also obtained from the PDB database and then processed by removing ions and water molecules through PyMol 2.4.0, resulting in PDB files. Consequently, regorafenib and RRM2 were translated to PDBQT format to find the active pocket. Finally, AutoDockTools 1.5.7 was used for molecular docking, and the results were visualized by Pymol. The binding energy of related active molecules was $\leqq -5.0$ kJ/mol, indicating that the molecules were well docked with the target and could bind spontaneously.

QUANTIFICATION AND STATISTICAL ANALYSIS

Statistical analysis was carried out by GraphPad Prism software. Data are represented as mean $\pm$ SEM. Statistical analysis between two groups were compared using unpaired two-tailed Student's t test. Statistics analysis among multiple groups were compared using one-way analysis of variance (ANOVA). *p* value <0.05 was considered to be significantly different.